

Structural visualization of polarization fatigue in epitaxial ferroelectric oxide devices

DAL-HYUN DO¹, PAUL G. EVANS^{1*}, ERIC D. ISAACS^{2†}, DONG MIN KIM¹, CHANG BEOM EOM¹ AND ERIC M. DUFRESNE³

¹Department of Materials Science and Engineering, University of Wisconsin, Madison, Wisconsin 53706, USA

²Bell Laboratories, Lucent Technologies, Murray Hill, New Jersey 07974, USA

³Department of Physics, University of Michigan, Ann Arbor, Michigan 48109, USA

†Present address: Center for Nanoscale Materials, Argonne National Laboratory, Argonne, Illinois 60439, USA

*e-mail: evans@engr.wisc.edu

Published online: 23 May 2004; doi:10.1038/nmat1122

Ferroelectric oxides, such as $\text{Pb}(\text{Zr,Ti})\text{O}_3$, are useful for electronic and photonic devices because of their ability to retain two stable polarization states, which can form the basis for memory and logic circuitry¹. Requirements for long-term operation of practical devices such as non-volatile RAM (random access memory) include consistent polarization switching over many (more than 10^{12}) cycles of the applied electric field, which represents a major challenge². As switching is largely controlled by the motion and pinning of domain walls, it is necessary to develop suitable tools that can directly probe the ferroelectric domain structures in operating devices—thin-film structures with electrical contacts. A recently developed synchrotron X-ray microdiffraction technique complements existing microscopic probes, and allows us to visualize directly the evolution of polarization domains in ferroelectric devices, through metal or oxide electrodes, and with submicrometre spatial resolution. The images reveal two regimes of fatigue, depending on the magnitude of the electric field pulses driving the device: a low-field regime in which fatigue can be reversed with higher electric field pulses, and a regime at very high electric fields in which there is a non-reversible crystallographic relaxation of the epitaxial ferroelectric film.

A common feature of ferroelectric capacitors (as, for example, in Fig. 1a) is a rapid decrease in the polarization that can be switched following many cycles of an applied electric field¹. In devices with elemental metal electrodes, this polarization fatigue has been linked to the migration of oxygen to the electrode–ferroelectric interface and the development of oxygen vacancy clusters that can inhibit the switching by pinning domain walls³. A second possibility involves the formation of layers at electrode interfaces that effectively reduce the total electric field applied across the device or inhibit the nucleation of oppositely polarized domains^{2,4}. These mechanisms modify the dynamics of ferroelectric domains in applied electric fields, and depend on the magnitude and frequency of the field as well as the details of the device preparation². Microscopy has shown that both polarization switching⁵ and the eventual evolution of fatigue in operating devices is inhomogeneous on the micrometre scale⁶. Structural measurements on ferroelectric devices have thus far been limited to either much larger

scales or, using transmission electron microscopy, to unfavourable sample geometries that complicate *in situ* observations during device operation. In comparison with techniques such as measurements of the piezoelectric response of the ferroelectric material with an atomic force microscope⁷, X-ray microdiffraction is a structural probe that does not require an electric field be applied during imaging and is not complicated by the mechanical properties of the sample⁸.

$\text{PbZr}_{1-x}\text{Ti}_x\text{O}_3$ (PZT) is an attractive material for ferroelectric devices because it has a large polarization, has the simple ABO_3 perovskite structure, and is reasonably straightforward to synthesize. We fabricated 200- μm -diameter PZT capacitors with Pt top electrodes on epitaxial thin-film multilayers (Fig. 1a). Images of the polarization within these devices were formed by scanning the sample in the focused X-rays, and monitoring the intensity of the PZT {002} Bragg reflections (Fig. 1b). Upon reversal of the stored polarization, we observed a 30% change in the intensity of PZT reflections, which formed the basis for our image contrast. The change in intensity is a crystallographic effect that is connected to the change in the index of the surface-normal *c*-axis X-ray reflection (for example from 002 to $0\bar{0}2$) that occurs during switching. Friedel's law ordinarily requires that intensities at reciprocal space points related by inversion (for example, hkl and $\bar{h}\bar{k}\bar{l}$) be equal, but does not apply in cases in which absorption is important⁹. This approach—using the intensity of X-ray reflections to distinguish oppositely polarized regions of ferroelectrics—has been widely used in the study of ferroelectric domains in bulk crystals of lithium niobate by X-ray topography, as well as in the determination of the absolute orientation of other materials with polar unit cells^{10–12}.

Images of a PZT device in the remnant polarization state, at zero applied voltage after the application of a voltage pulse, were taken for both stable polarization states. We first established that X-ray microdiffraction was an accurate probe of the local stored ferroelectric polarization. By applying voltage pulses to the bottom electrode, the PZT thin film was switched between stored polarization states in which the [001] and $[0\bar{0}\bar{1}]$ directions were normal to the device surface. Images of a region including the edge of an electrode (Fig. 1c) show the effect of switching the remnant polarization on the intensity of the X-ray

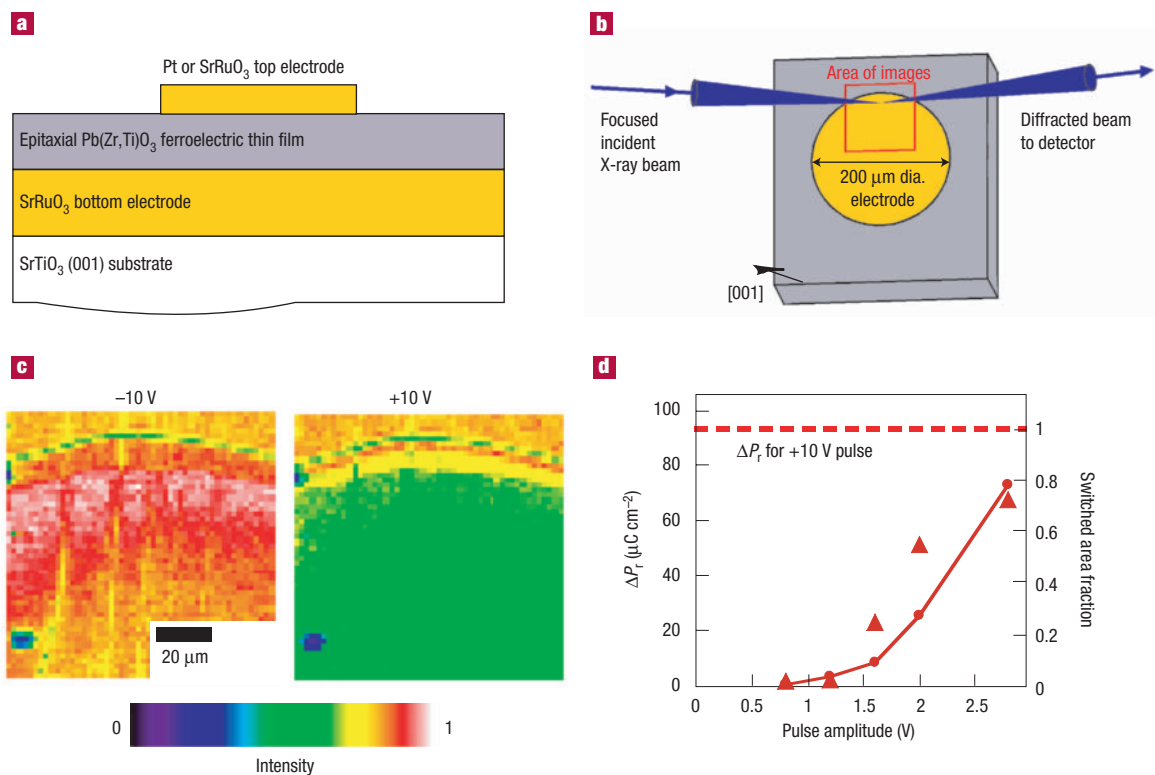


Figure 1 Polarization switching in a PZT thin-film capacitor. **a**, Epitaxial ferroelectric capacitor fabricated on an (001) oriented SrTiO₃ substrate. **b**, A diagram of the synchrotron X-ray microdiffraction experiment. **c**, Real-space images of the intensity of the (002) reflection of Pb(Zr,Ti)O₃ following -10 V and $+10$ V pulses to the bottom electrode of the capacitor device. The intensity of the X-ray reflection varies with the local ferroelectric polarization, and changes by 30% upon polarization switching. Each image required ~ 30 min to acquire. **d**, The area of the region in which the intensity has changed (triangles) and the total switched polarization ΔP_r (solid line) are proportional, and provide independent observations of the switching process. There was no change in the intensity of the (002) reflection in the area of the PZT film not covered by the top electrode.

reflection from the film. No evolution of images with time was observed in repeated scans of the same area. (Long-term exposure to the beam, however, with total incident flux of the order of 10^{12} – 10^{13} photons μm^{-2} , caused permanent beam damage to the PZT film.) The mean intensity

of the reflection from the device area is 30% greater following a -1.25 MV cm^{-1} triangular electric field pulse of 500 μs duration to the bottom electrode than for an identical positive pulse. By following -1.25 MV cm^{-1} pulses with positive voltage pulses of amplitudes near

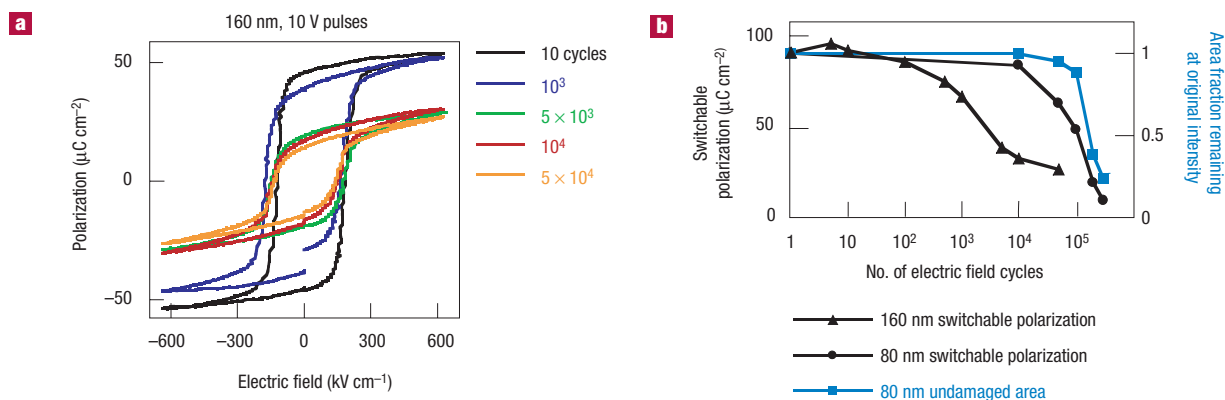


Figure 2 Polarization fatigue. **a**, Polarization–electric-field hysteresis loops for the 160 nm PZT thin film exhibit polarization fatigue after $\sim 10^4$ electric field cycles. **b**, When operated at the same voltage, capacitors fabricated from 80 nm thin films (squares) required a factor of roughly 10^2 more cycles to be fatigued to the same remnant polarization as those fabricated from 160 nm PZT layers. The evolution of the area of regions of reduced (002) reflection intensity measured from the images of Fig. 4 is consistent with the decrease in switchable polarization.

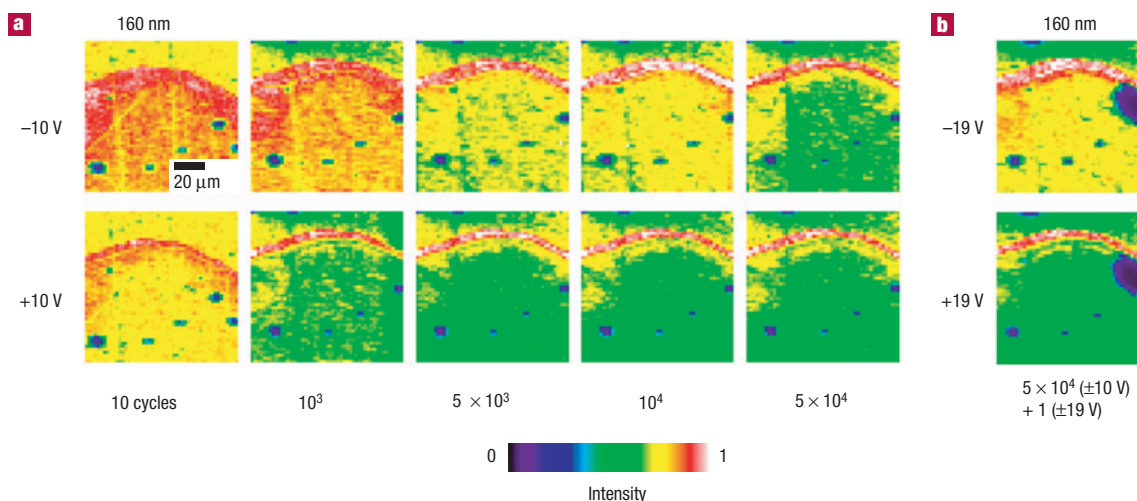


Figure 3 Low-field fatigue. **a**, Images of the evolution of the intensity of the PZT (002) reflection in a 160-nm-thick film during fatigue under low electric field conditions. The film is eventually pinned in the state that would normally follow a positive voltage pulse to the bottom electrode. **b**, An electric field pulse of a larger magnitude restores the switchable polarization.

the coercive field, we found that the polarization was switched in discrete areas of the film and that the switched area in the X-ray microdiffraction images was proportional to the net reversal of the stored polarization (Fig. 1d). Apart from the overall change in intensity, rocking curves and θ - 2θ scans showed no difference between the two polarization states.

The development of polarization fatigue resulted in the collapse of the polarization–electric-field hysteresis loops upon repeated cycling of the applied electric field. Using 1 kHz triangle wave fields, we found that after a number of cycles the switchable polarization rapidly decreased from an initial value of $95 \mu\text{C cm}^{-2}$ (Fig. 2a). The onset of fatigue occurred in two qualitative regimes. At pulse amplitudes of 10 V applied to the 160-nm-thick PZT films (a nominal field of 625 kV cm^{-1}), fatigue occurred within 10^4 cycles and an eventual decrease of the switchable polarization to $25 \mu\text{C cm}^{-2}$ was observed (Fig. 2b). Microdiffraction maps of the rapid fatigue process in this low-electric-field regime show that as a result of fatigue the PZT layer gradually becomes pinned in the state that would normally be reached by applying a positive voltage to the bottom electrode. Figure 3a shows the evolution of the intensity of the X-ray reflections in pairs of images taken following positive and negative voltage pulses at interruptions in cycling the electric field after increasing numbers of cycles.

The low-field fatigue process preserves the crystal structure of the PZT layer, but pins it in a state in which it can no longer respond to applied voltage pulses. Larger-amplitude voltage pulses (up to $\pm 19 \text{ V}$, 1.2 MV cm^{-1}) restored the switchable polarization observable both in X-ray images and electrical measurements (Fig. 3b). It has been observed previously that larger fields may be sufficient to allow the nucleation of domains or to de-pin domain walls when switching at lower voltages is suppressed^{2,13,14}.

It has often been observed that fatigue is delayed in devices using complex oxide rather than elemental metal electrodes¹⁵. In previous studies, SrRuO₃ (SRO) top electrode layers have delayed the onset of fatigue to the order of 10^{10} or more cycles¹⁶. We found that the low-field mechanism of fatigue was not observed in up to 5×10^7 electric field cycles in devices fabricated using SRO rather than Pt top electrodes, suggesting a chemical driving force for low-field fatigue, such as the oxygen vacancy mechanism proposed previously³. The development of

fatigue and the clear preference for a single polarization state in devices with Pt top electrodes suggest that the asymmetry of the electrode composition (that is, epitaxial SRO bottom electrodes versus Pt top electrodes) is important. However, we observed only a slight shift in the coercive field (by -0.2 V , or 12.5 kV cm^{-1}) during the fatigue process, indicating that the applied fields were well above the effective coercive fields and that low-field fatigue originated in either pinning of domain motion or the effective suppression of nucleation². In addition, hysteresis loops retained a sharp transition at the coercive field throughout the fatigue process. The fatigue mechanism is thus not simply a gradual development of imprint in local areas of the film.

The origin of polarization fatigue is very different in measurements made at higher electric fields. With pulse amplitudes of 1.2 MV cm^{-1} , resulting from 19 V pulses applied to a 160 nm film or 10 V across an 80 nm film, the onset of fatigue occurred after 2×10^5 or more cycles of the field (Fig. 2b), a factor of $\sim 10^2$ more than at lower fields. Fatigue at high electric fields was accompanied by a much larger eventual decrease in the switchable polarization accompanied by a marked structural change in the PZT thin film. No rejuvenation with higher fields was possible. Fields of this magnitude are a factor of 2–3 higher than those typically applied to capacitor devices, and represent the high-field limit of polarization fatigue. For a small number of cycles, the result of switching at high fields is similar to what is observed at low fields: the PZT film switches uniformly between polarization states. As fatigue develops in the high-field case, however, the X-ray reflections in some areas of the film decrease in intensity by a factor of up to ten. These regions, which are at first isolated, coalesce at larger numbers of polarization cycles, and eventually cover the entire area beneath the electrodes (Fig. 4). The fraction of the area of the device occupied by these regions of drastically reduced intensity increases as fatigue develops, and scales with the decrease in the switchable polarization (Fig. 2b). In the areas of the film initially unaffected by fatigue, there was no reduction in the intensity difference between states prepared by positive and negative pulses. The failure of devices fabricated from 160 nm PZT layers in the high-electric-field regime was more marked, resulting in damage to the device that was visible under an optical microscope. High-field fatigue was distinct from the process of

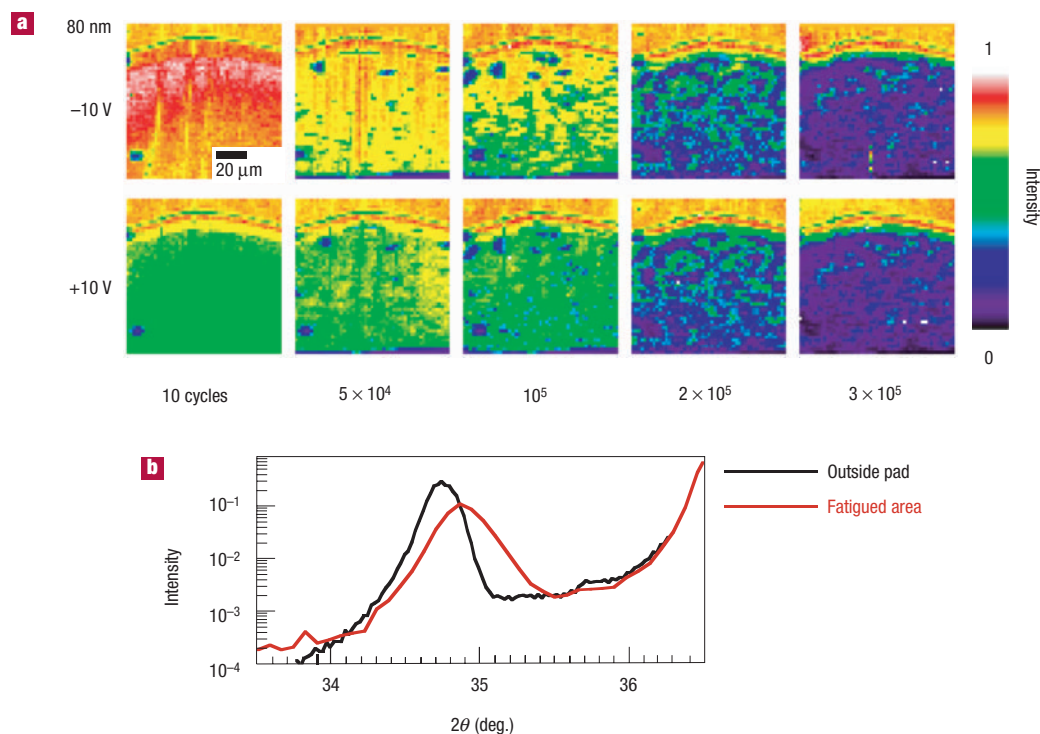


Figure 4 High-field fatigue. **a**, The evolution of polarization fatigue in an 80-nm-thick film under high fields occurs by the development and spread of areas of reduced X-ray reflection intensity. **b**, The PZT (002) reflection is shifted to smaller lattice constant in these areas, consistent with the relaxation of the strain resulting from epitaxial growth.

catastrophic shorting of these devices, which occurred at still higher electric fields.

The structural effect of polarization fatigue at high electric fields is also clear in reciprocal space. We have already noted the factor-of-ten decrease in the intensity of reflections at the as-grown lattice spacing of the PZT film. In addition, following high-field fatigue, the PZT (002) reflection is broader in reciprocal space scans along [00 $\bar{1}$] and in rocking curve measurements. For the thinner films, which are under strain following growth, the peak intensity of the PZT reflection is shifted during the high-field fatigue process to higher 2θ angle, corresponding to a 0.3% decrease in the PZT out-of-plane lattice constant (Fig. 4b) and a shift towards the bulk lattice parameter. The thicker, 160 nm films were fully relaxed before fatigue and exhibited the decrease in intensity, but only a slight shift in the reciprocal space position of the (002) reflection. The structural changes may be related to the formation of defects relaxing the epitaxial strain, or to the accumulation of oxygen vacancies in increasingly thick regions near the Pt electrode¹⁷. Because our sampling of the diffraction pattern was limited to the vicinity of a single point in reciprocal space (Fig. 4b), the subtle structural changes with low-field fatigue as observed in ref. 18 in an X-ray crystal truncation rod measurement cannot be ruled out.

These X-ray microdiffraction measurements confirm previous suggestions that there are several important mechanisms of fatigue, and show that multiple mechanisms can simultaneously be important to an individual device. Recently, area-averaged dielectric loss measurements have also suggested that multiple mechanisms can be at work simultaneously¹⁹. In our case, the development of a single polarization state at low fields without a general shift in the coercive electric field suggests that the nucleation and growth of domains of the opposite polarization is suppressed. If domain wall pinning is the origin of this fatigue process, the motion of domain walls is ultimately hindered at

scales smaller than our X-ray spot size. At high fields, the fatigue process is irreversible and results in a drastic reduction of structural order in the PZT film. The structural understanding and control of fatigue presents an important continuing challenge to the realization of microelectronic and photonic devices based on ferroelectric oxide materials. X-ray microdiffraction is the ideal tool for understanding these and other complex phenomena in which structural, electronic and even magnetic effects are intertwined.

METHODS

Before PZT films were deposited, epitaxial SRO bottom electrodes were deposited on single crystal (001) SrTiO₃ substrates by off-axis radio-frequency (RF) magnetron sputtering²⁰. The epitaxial PZT films were grown on these electrodes by on-axis RF magnetron sputtering. The composition of the films, $x=0.55$, was chosen to be on the tetragonal side of the morphotropic phase boundary separating tetragonal and rhombohedral structural phases of PZT²¹. Polycrystalline platinum thin-film top electrodes were deposited by magnetron sputtering through a shadow mask defining 200- μ m-diameter capacitor devices. In order to avoid complications caused in measurements with insufficient electric field or pulse duration, the electrical waveforms for hysteresis loop and fatigue measurements were identical²². We used X-ray microdiffraction based on Fresnel zone plate focusing optics^{23,24} to differentiate between two regimes of electric field amplitude in the development of fatigue in epitaxially grown ferroelectric devices. A 10 keV X-ray beam from the 7ID beamline of the Advanced Photon Source was focused to an 800 nm spot and easily penetrated the top electrode, allowing electrical measurements to be carried out *in situ* without removing the sample from the diffractometer. The X-ray penetration length is of the order of several micrometres or more in our capacitor devices, and thus our measurements effectively average through the depth of the PZT film.

Received 4 November 2003; accepted 19 March 2004; published 23 May 2004.

References

1. Scott, J. F. *Ferroelectric Memories* (Springer, Berlin, 2000).
2. Tagantsev, A. K., Stolichnov, I., Colla, E. L. & Setter, N. Polarization fatigue in ferroelectric films: Basic experimental findings, phenomenological scenarios, and microscopic features. *J. Appl. Phys.* **90**, 1387–1402 (2001).
3. Dawber, M. & Scott, J. F. A model for fatigue in ferroelectric perovskite thin films. *Appl. Phys. Lett.* **76**, 1060–1062 (2000).

4. Larsen, P. K., Dormans, G. J. M., Taylor, D. J. & van Veldhoven, P. J. Ferroelectric properties and fatigue of $\text{PbZr}_{0.51}\text{Ti}_{0.49}\text{O}_3$ thin films of varying thickness: Blocking layer model. *J. Appl. Phys.* **76**, 2405–2413 (1994).
5. Nagarajan, V. *et al.* Dynamics of ferroelastic domains in ferroelectric thin films. *Nature Mater.* **2**, 43–47 (2002).
6. Colla, E. L. *et al.* Direct observation of region by region suppression of the switchable polarization (fatigue) in $\text{Pb}(\text{Zr}, \text{Ti})\text{O}_3$ thin film capacitors with Pt electrodes. *Appl. Phys. Lett.* **72**, 2763–2765 (1998).
7. Gruverman, A., Auciello, O. & Tokumoto, H. Imaging and control of domain structures in ferroelectric thin films via scanning force microscopy. *Annu. Rev. Mater. Sci.* **28**, 101–123 (1998).
8. Rogan, R. C., Tamura, N., Swift, G. A. & Üstündag, E. Direct measurement of triaxial strain fields around ferroelectric domains using X-ray microdiffraction. *Nature Mater.* **2**, 379–381 (2003).
9. James, R. W. *The Optical Principles of X-ray Diffraction* 33 (Cornell Univ. Press, Ithaca, New York, 1965).
10. Wallace, C. A. The display of twinning in lithium niobate by x-ray diffraction topography. *J. Appl. Crystallogr.* **3**, 546–547 (1970).
11. Vreeland, T. & Speriou, V. S. in *Applications of X-ray Topographic Methods to Materials Science* (eds Balibar, F. & Petroff, J.-F.) 501–509 (Plenum, New York, 1984).
12. Coster, D., Knol, K. S. & Prins, J. A. Difference in the intensities of x-ray reflection from the two sides of the 111 plane of zinc blende. *Z. Phys.* **63**, 345–369 (1930).
13. Colla, E. L., Tagantsev, A. K., Taylor D. V. & Kholkin, A. L. Fatigued state of the Pt-PZT-Pt system. *Integr. Ferroelectr.* **18**, 19–28 (1997).
14. Scott, J. F. & Pouligny, B. J. Raman spectroscopy of submicron KNO_3 films. II. Fatigue and space-charge effects. *J. Appl. Phys.* **64**, 1547–1561 (1988).
15. Auciello, O. *et al.* Review of composition-structure-property relationships for PZT-based heterostructure capacitors. *Integr. Ferroelectr.* **6**, 173–187 (1995).
16. Eom, C. B. *et al.* Fabrication and properties of epitaxial ferroelectric heterostructures with (SrRuO_3) isotropic metallic oxide electrodes. *Appl. Phys. Lett.* **63**, 2570–2572 (1993).
17. Duiker, H. M. *et al.* Fatigue and switching in ferroelectric memories: theory and experiment. *J. Appl. Phys.* **68**, 5783–5791 (1990).
18. Thompson, C. *et al.* X-ray scattering evidence for the structural nature of fatigue in epitaxial $\text{Pb}(\text{Zr}, \text{Ti})\text{O}_3$ films. *Appl. Phys. Lett.* **78**, 3511–3513 (2001).
19. Jiang, A. *et al.* Studies of switching kinetics in ferroelectric thin films. *Jpn. J. Appl. Phys.* **42**, 6973–6982 (2003).
20. Eom, C. B. *et al.* Single-crystal epitaxial thin films of the isotropic metallic oxides $\text{Sr}_{1-x}\text{Ca}_x\text{RuO}_3$ ($0 \leq x \leq 1$). *Science* **258**, 1766–1769 (1992).
21. Noheda, B. *et al.* A monoclinic ferroelectric phase in the $\text{Pb}(\text{Zr}_{1-x}\text{Ti}_x)\text{O}_3$ solid solution. *Appl. Phys. Lett.* **74**, 2059–2061 (1999).
22. Grossmann, M. *et al.* Correlation between switching and fatigue in $\text{PbZr}_{0.3}\text{Ti}_{0.7}\text{O}_3$ thin films. *Appl. Phys. Lett.* **77**, 1894–1896 (2000).
23. Cai, Z., Lai, B., Xiao, Y. & Xu, S. An X-ray diffraction microscope at the Advanced Photon Source. *J. Phys. IV* **104**, 17–20 (2003).
24. Lai, B. *et al.* Hard X-ray phase zone plate fabricated by lithographic techniques. *Appl. Phys. Lett.* **61**, 1877–1879 (1992).

Acknowledgements

This work was supported by the National Science Foundation through the University of Wisconsin Materials Research Science and Engineering Center (grant number DMR-0079983) and grant no. DMR-0313764 (C.B.E.). Use of the Advanced Photon Source was supported by the US Department of Energy, Office of Science, Office of Basic Energy Sciences (contract number W-31-109-Eng-38). E.D. acknowledges support from the US Department of Energy (grant numbers DE-FG02-03ER46023 and DE-FG02-00ER15031), and from the NSF FOCUS physics frontier centre. Correspondence and requests for materials should be addressed to P.G.E.

Competing financial interests

The authors declare that they have no competing financial interests.